

Absolute Measurements of Total Peroxy Nitrate Mixing Ratios by Thermal Dissociation Blue Diode Laser Cavity Ring-Down Spectroscopy

Dipayan Paul and Hans D. Osthoff*

Department of Chemistry, University of Calgary, 2500 University Drive NW, Calgary AB T2N 1N4, Canada

Peroxy-carboxylic nitric anhydrides (PANs) have long been recognized as important trace gas constituents of the troposphere. Here, we describe a blue diode laser thermal dissociation cavity ring-down spectrometer for rapid and absolute measurements of total peroxyacyl nitrate (Σ PAN) abundances at ambient concentration levels. The PANs are thermally dissociated and detected as NO_2 , whose mixing ratios are quantified by optical absorption at 405 nm relative to a reference channel kept at ambient temperature. The effective NO_2 absorption cross-section at the diode laser emission wavelength was measured to be $6.1 \times 10^{-19} \text{ cm}^2 \text{ molecule}^{-1}$, in excellent agreement with a prediction based on a projection of a high-resolution literature absorption spectrum onto the laser line width. The performance, i.e., accuracy and precision of measurement and matrix effects, of the new 405 nm thermal dissociation cavity ring-down spectrometer was evaluated and compared to that of a 532 nm thermal dissociation cavity ring-down spectrometer using laboratory-generated air samples. The new 405 nm spectrometer was considerably more sensitive and compact than the previously constructed version. The key advantage of laser thermal dissociation cavity ring-down spectroscopy is that the measurement can be considered absolute and does not need to rely on external calibration.

Peroxy-carboxylic nitric anhydrides, commonly referred to by their non-IUPAC name peroxyacyl nitrates (PANs; general structure $\text{RC(O)O}_2\text{NO}_2$, where R is typically an alkyl group), have long been recognized as important trace gas constituents of the troposphere.^{1,2} Of the more than 43 different PANs that have been detected in ambient air so far, peroxyacetic nitric anhydride (usually called peroxyacetyl nitrate or PAN, $\text{CH}_3\text{C(O)O}_2\text{NO}_2$) is usually the most abundant PAN species and often also the most abundant odd nitrogen ($\text{NO}_y \equiv \text{NO} + \text{NO}_2 + \text{NO}_3 + 2\text{N}_2\text{O}_5 + \Sigma\text{PANs} + \Sigma\text{RONO}_2 + \text{HNO}_3 + \text{HONO} + \text{ClONO}_2 + \dots$). The PANs are formed as byproducts in the same photochemistry between NO_x ($\equiv \text{NO} + \text{NO}_2$) and volatile organic compounds (VOCs) that produces ozone in the troposphere; the relative

abundances of the various PANs thus contain information on the VOCs involved in the ozone-formation process. PANs are susceptible to thermal dissociation, but are quite stable in the middle and upper troposphere as direct photolysis and OH-initiated degradation reactions are slow.³ As a consequence, PANs can act as NO_x reservoir species and be transported over long distances, slowly releasing NO_x in the form of NO_2 and affecting ozone production in the remote troposphere.^{1,2}

Over the years, a variety of techniques have been used to quantify the mixing ratios of PANs in ambient air. The most commonly used technique is gas chromatography with electron capture detection (GC-ECD). With capillary columns and online preconcentration, GC-ECD can achieve a limit of detection of a few parts per trillion by volume (pptv, 10^{-12} , v/v), and column run times of less than 1 min are possible.⁴ Electron capture detectors are prone to interference from halogenated species and oxygen and exhibit different response factors for different PANs; in an alternative method, PANs are detected by post-column thermal dissociation to NO_2 (reaction 1), which is quantified by either luminol chemiluminescence⁵ or luminol chemiluminescence coupled to peroxy radical chemical amplification.⁶



Recently, thermal dissociation chemical ionization mass spectrometry (TD-CIMS) using I^- reagent ion has been used to measure PANs in ambient air.⁷ In TD-CIMS, the PANs are dissociated in a heated inlet (reaction 1), and the generated peroxy radicals, RC(O)O_2 , are reacted with I^- reagent ion to form the corresponding carboxylate anions, which are monitored by negative ion mass spectrometry:⁷



(3) Talukdar, R. K.; Burkholder, J. B.; Schmoltner, A. M.; Roberts, J. M.; Wilson, R. R.; Ravishankara, A. R. *J. Geophys. Res., [Atmos.]* **1995**, *100*, 14163–14173.

(4) Flocke, F. M.; Weinheimer, A. J.; Swanson, A. L.; Roberts, J. M.; Schmitt, R.; Shertz, S. J. *Atmos. Chem.* **2005**, *52*, 19–43.

(5) Blanchard, P.; Shepson, P. B.; So, K. W.; Schiff, H. I.; Bottenheim, J. W.; Gallant, A. J.; Drummond, J. W.; Wong, P. *Atmos. Environ., Part A* **1990**, *24*, 2839–2846.

(6) Blanchard, P.; Shepson, P. B.; Schiff, H. I.; Drummond, J. W. *Anal. Chem.* **1993**, *65*, 2472–2477.

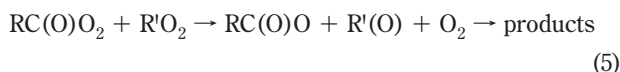
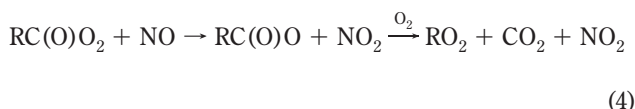
(7) Slusher, D. L.; Huey, L. G.; Tanner, D. J.; Flocke, F. M.; Roberts, J. M. *J. Geophys. Res., [Atmos.]* **2004**, *109*, D19315.

* To whom correspondence should be addressed. E-mail: hosthoff@ucalgary.ca. Phone: (403) 220-8689. Fax: (403) 289-9488.

(1) Roberts, J. M. *Atmos. Environ., Part A* **1990**, *24*, 243–287.

(2) Roberts, J. M. In *Volatile Organic Compounds in the Atmosphere*; Koppmann, R., Ed.; Blackwell Publishing: Oxford, UK, 2007; pp 221–268.

The detection limits (<1 pptv) and instrument response times (<1 s) of TD-CIMS instruments are superb; however, the technique requires the use of an internal standard (usually ^{13}C -labeled PAN) to track matrix effects, as the instrument response depends on the ambient mixing ratios of NO_2 , NO , and other peroxy radicals, which can (partially) destroy the peroxy radicals generated in the heated inlet:



An alternative to quantifying individual PANs is measurement of *total* peroxyacyl nitrate (ΣPAN) abundances. In this method, the sampled PANs are dissociated directly (as a group) to NO_2 in a heated inlet, skipping the time-consuming steps of preconcentration and separation on a GC column. The common dissociation product, NO_2 , is quantified by either laser-induced fluorescence (LIF)^{8,9} or cavity ring-down spectroscopy (CRDS)¹⁰ relative to an unheated reference channel. Measurement of ΣPAN is preferred when the goal is to track the partitioning of odd nitrogen; however, since the method lacks specificity, no information is gained on the VOCs involved in the ozone-formation process.

The electron capture, CIMS, and LIF detectors need to rely on external calibration, which involves laborious synthesis, purification, and storage of PAN standards and use of diffusion sources. We have recently reported thermal dissociation cavity ring-down spectroscopy (TD-CRDS) measurements of ΣPAN in laboratory-generated air samples which utilized a pulsed, Nd:YAG laser (532 nm) to quantify NO_2 .¹⁰ The main advantage of TD-CRDS is that it does not require calibration since the measurement principle is optical absorption; however, it does require knowledge of the relevant NO_2 absorption cross-section and accurate calibration of flow meters, pressure transducers, and thermocouples and characterization of the PAN conversion efficiency in the heated inlet.¹⁰ At 532 nm, quantification of NO_2 is subject to interference from optical absorption by O_3 .¹¹ For measurements of ΣPAN , the O_3 interference does not pose a problem as O_3 does not thermally dissociate in the quartz inlet heated to 250 °C, such that its contribution to the optical absorption is the same in both the sample and reference channels.¹⁰

Several groups have recently reported on the use of continuous-wave (cw) blue diode laser CRDS to quantify NO_2 .^{12–16} The use of blue diode lasers is attractive for a variety of reasons: At 405 nm, the absorption cross-section of NO_2 is increased (by a factor of about 4) and that of ozone is greatly reduced, such that interference-free and more sensitive measurements of NO_2 are possible. The only potentially interfering species at 405 nm are glyoxal and methylglyoxal, but these are usually not present in sufficiently high concentration in the atmosphere to be significant. Another advantage of blue diode lasers is the ease with which they can be coupled to the ring-down cavity, because their emission profiles are typically rather broad. Finally, diode lasers are considerably less expensive and more compact than Nd:YAG lasers and easier to maintain. One potential disadvantage is the larger Rayleigh scattering cross-section in the blue region of the visible spectrum, which is also dependent on relative humidity.¹²

In this paper, we describe a new cw blue diode laser thermal dissociation cavity ring-down spectrometer for measurement of ΣPAN abundances. The performance of the new 405 nm TD-CRDS instrument is compared to that of the 532 nm TD-CRDS instrument described earlier.¹⁰ Inlet matrix effects are evaluated by sampling a gas stream of PAN or peroxypropionic nitric anhydride (PPN) eluted from a capillary diffusion source to which NO , NO_2 , ozone, or water vapor has been added. The output of the diffusion source was also monitored by a $\text{NO}-\text{O}_3$ chemiluminescence analyzer. Applications and limitations of the new TD-CRDS instrument are discussed.

EXPERIMENTAL SECTION

Measurements of ΣPAN by Pulsed Nd:YAG Laser Cavity Ring-Down Spectroscopy. The Nd:YAG TD-CRDS has instrument been described in detail elsewhere,¹⁰ but is briefly described here since the blue diode TD-CRDS instrument “inherited” many of its components. The Nd:YAG instrument uses two cells: One serves as a reference channel and is used to monitor (background) NO_2 mixing ratios, and the other utilizes a heated inlet consisting of a 1/4 in. outer diameter (o.d.) quartz tube heated to 250 °C to quantitatively dissociate PANs to NO_2 (reaction 1). The heated quartz tube is connected to the sample CRDS cell via a short section of 1/4 in. o.d. PFA Teflon tubing heated to 75 °C. A Teflon “turbulator”¹⁷ placed inside this tubing ensures a uniform temperature profile within the ring-down cavity. The sample CRDS cell was maintained at a temperature of 49 °C, while the reference cell was at room temperature.

The CRDS cells were constructed from 3/8 in. o.d., 5/16 in. inner diameter (i.d.) PFA Teflon held in place by a custom-built aluminum enclosure. The CRDS mirrors (Advanced Thin Films, manufacturer-specified reflectivity $R = 99.9998\%$, 2.54 cm diam-

(8) Day, D. A.; Wooldridge, P. J.; Dillon, M. B.; Thornton, J. A.; Cohen, R. C. *J. Geophys. Res. [Atmos.]* **2002**, *107*, D64046.

(9) Wooldridge, P. J.; Perring, A. E.; Bertram, T. H.; Flocke, F. M.; Roberts, J. M.; Singh, H. B.; Huey, L. G.; Thornton, J. A.; Wolfe, G. M.; Murphy, J. G.; Fry, J. L.; Rollins, A. W.; LaFranchi, B. W.; Cohen, R. C. *Atmos. Meas. Tech.* **2010**, *3*, 593–607.

(10) Paul, D.; Furgeson, A.; Osthoff, H. D. *Rev. Sci. Instrum.* **2009**, *80*, 114101.

(11) Osthoff, H. D.; Brown, S. S.; Ryerson, T. B.; Fortin, T. J.; Lerner, B. M.; Williams, E. J.; Pettersson, A.; Baynard, T.; Dube, W. P.; Ciciora, S. J.; Ravishankara, A. R. *J. Geophys. Res., [Atmos.]* **2006**, *111*, D12305.

(12) Fuchs, H.; Dubé, W. P.; Lerner, B. M.; Wagner, N. L.; Williams, E. J.; Brown, S. S. *Environ. Sci. Technol.* **2009**, *43*, 7831–7836.

(13) Mazurenka, M. I.; Fawcett, B. L.; Elks, J. M. F.; Shallcross, D. E.; Orr-Ewing, A. J. *Chem. Phys. Lett.* **2003**, *367*, 1–9.

(14) Wada, R.; Orr-Ewing, A. J. *Analyst* **2005**, *130*, 1595–1600.

(15) Courtillot, I.; Morville, J.; Motto-Ros, V.; Romanini, D. *Appl. Phys. B: Lasers Opt.* **2006**, *85*, 407–412.

(16) Hargrove, J.; Wang, L. M.; Muyskens, K.; Muyskens, M.; Medina, D.; Zaide, S.; Zhang, J. S. *Environ. Sci. Technol.* **2006**, *40*, 7868–7873.

(17) Fuchs, H.; Dubé, W. P.; Ciciora, S. J.; Brown, S. S. *Anal. Chem.* **2008**, *80*, 6010–6017.

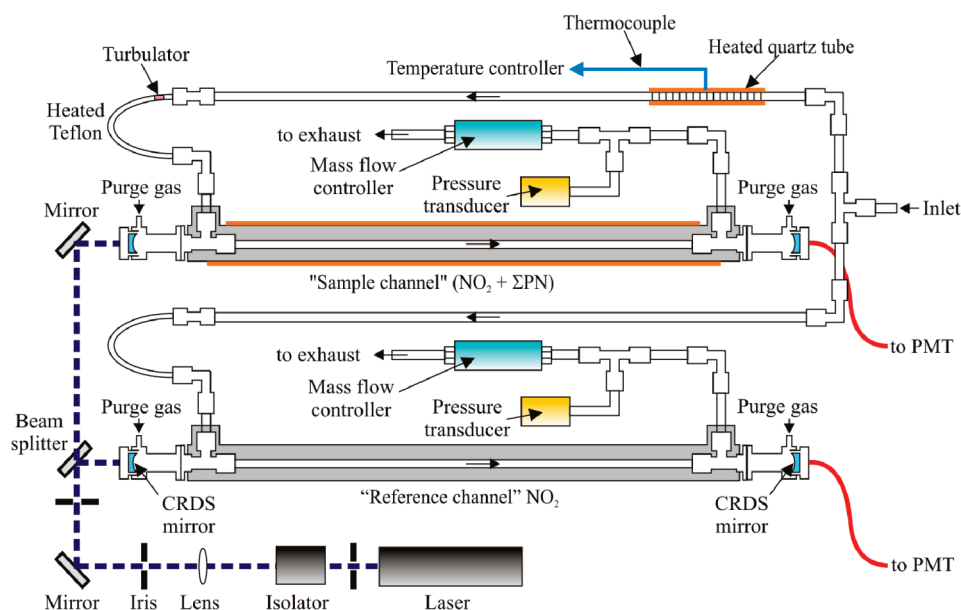


Figure 1. Schematic of the blue diode laser TD-CRDS instrument. For a discussion, see the text.

eter) are seated in custom-built mirror holders 111 cm apart. The mirrors are protected from contamination by a small flow (~ 50 standard cubic centimeters per minute, sccm) of ultrapure (“zero”) air. The ratio of the distance between the CRDS mirrors to the distance over which sample air is present in this instrument is $R_L = 1.21$ (calculated from the physical dimensions of the sample cell and assuming no mixing of sample gas into the purge volume).

Each channel was operated with a mass flow rate of 2.5 standard liters per minute (slpm), controlled by a pair of mass flow controllers (Celerity Unit 180). A flow restriction placed at the tip of the common inlet results in sample cell pressures of 450 and 530 Torr, respectively, monitored by a pair of pressure transducers (MKS Baratron 722A) whose output was digitized at a sampling rate of 1 kHz.

Mixing ratios of background NO_2 , and background NO_2 plus NO_2 generated from PAN thermal dissociation, are monitored by optical absorption at 532 nm.¹¹ Light from a pulsed Nd:YAG laser (Big Sky Laser, Ultra 20) operated at a 20 Hz repetition rate is coupled into the optical cavity via an optical isolator and turning mirrors (Figure 1). Light exiting the optical cavities is focused by collimating optics onto multimode fibers; the output at the other end of the fibers illuminates a pair of photomultiplier tubes (PMTs; Hamamatsu H9433-03MOD) which have a bandwidth of 10 MHz. For the work presented here, the voltage output of the two PMTs was digitized using a 1 MHz (aggregate) data acquisition card (National Instrument USB-6251) triggered by the “TTL-sync” output of the Nd:YAG laser and connected to a laptop computer via a universal serial bus (USB) port. Parameters of a first-order exponential curve were fitted to the observed decay traces immediately after acquisition using software written in LabVIEW. The $1/e$ ring-down time constants of 20 consecutive decay traces were averaged to produce 1 s data.

Concentrations of NO_2 are derived using

$$N = \frac{R_L}{\sigma c} \left(\frac{1}{\tau_{\text{sample}}} - \frac{1}{\tau_0} \right) \quad (6)$$

where N is the number density of NO_2 in the sample gas, σ is the NO_2 absorption cross-section (we used the value revised by Fuchs et al., $1.51 \times 10^{-19} \text{ cm}^2 \text{ molecule}^{-1}$),¹⁸ c is the speed of light, τ is the ring-down time constant in the presence of the absorber, and τ_0 is the ring-down time constant in its absence. The concentrations were further corrected for dilution by the purge flow and converted to mixing ratios using the ideal gas law.

Mixing ratios of peroxyacyl nitrates are quantified by the difference between the sample and reference channels. Since the NO_2 absorption cross-section is slightly pressure- and temperature-dependent,¹⁹ measurements of the heated sample cell were scaled to that of the room-temperature reference cell; the scaling factor was determined from the slope observed when sampling up to 100 ppb by volume (ppbv, 10^{-9}) of NO_2 in zero air. The scaling factor (sample/reference) in the 532 nm instrument is approximately 1.03 and also removes any systematic differences between the two cells arising from differences in the pressure, temperature, and flow calibrations, thus making the difference measurement more accurate and robust.¹⁰

The detection limit (2σ) of the Nd:YAG TD-CRDS instrument in these experiments was 200 pptv in a 1 s average time. The (slope) accuracy was approximately 4% limited mainly by uncertainties in the knowledge of the NO_2 absorption cross-section.^{11,18} The PAN to NO_2 conversion efficiency was found to be quantitative (as judged by simultaneous measurements using a commercial NO_y monitor) from the detection limit to about 10 ppbv. Hence, the TD-CRDS linear dynamic range extends

(18) Fuchs, H.; Ball, S. M.; Bohn, B.; Brauers, T.; Cohen, R. C.; Dorn, H. P.; Dubé, W. P.; Fry, J. L.; Häsel, R.; Heitmann, U.; Jones, R. L.; Kleffmann, J.; Mentel, T. F.; Müsgen, P.; Rohrer, F.; Rollins, A. W.; Ruth, A. A.; Kiendler-Scharr, A.; Schlosser, E.; Shillings, A. J. L.; Tillmann, R.; Varma, R. M.; Venables, D. S.; Villena Tapia, G.; Wahner, A.; Wegener, R.; Wooldridge, P. J.; Brown, S. S. *Atmos. Meas. Tech.* **2010**, *3*, 21–37.

(19) Vandaele, A. C.; Hermans, C.; Fally, S.; Carleer, M.; Merienne, M. F.; Jenouvrier, A.; Coquart, B.; Colin, R. J. *Quant. Spectrosc. Radiat. Transfer* **2003**, *76*, 373–391.

over the same range.¹⁰ For PAN measurements above a mixing ratio of 10 ppbv in ultrapure, or zero, air, the TD-CRDS data need to be corrected due to the recombination reaction (3) which occurs in the sample channel (eq 7b in ref 10).

Blue Diode Laser Cavity Ring-Down Spectrometer for Measurements of Σ PAN. The blue diode laser TD-CRDS instrument was used in two different configurations: as a stand-alone version and another for comparison with the Nd:YAG laser system described further below.

In the stand-alone version, the instrument resembled the diagram shown in Figure 1. The flow rates and the design of the CRDS sample cells were identical to those of the Nd:YAG system. Optics, i.e., CRDS mirrors (Advanced Thin Films, manufacturer-specified reflectivity $R = 99.9983\%$), turning mirrors, and beam splitters (CVI), with maximum reflectivity at 405 nm, were used. In addition, band-pass filters (405 ± 10 nm, Thorlabs) were placed between the PMTs and the optical fiber collecting the ring-down signal as a precaution as no significant difference was observed when these were removed.

The self-contained blue diode laser module was purchased from Power Technologies (model IQu2A105(405-120)G26/8983). It features 120 mW single-mode and circular output (manufacturer-specified beam size 1.08 mm), analog external modulation, and thermoelectric temperature control. Its output was modulated using an external square-wave function generator (SRS Instruments DS 335, manufacturer-specified fall-time of <15 ns) operated at a frequency of 750 Hz and modulation amplitude of either 0.5 or 1.0 V, with the lower voltage at 0 V (i.e., zero output intensity). Since the fall time of the laser diode output is faster than could be measured with our data acquisition system (operated at 2.5 MHz), no additional buildup of light occurs in the optical cavity during the ring-down decay. Higher modulation rates (in excess of 1 kHz) were possible but were avoided as the ring-down decay traces tended to "bunch up"; i.e., the laser intensity would begin to increase again before the intensity of the previous ring-down decay had returned to the baseline. Accurate knowledge of the PMT zero offset, or "baseline", is required for accurate fitting of the ring-down decay traces; in the LabVIEW software, the offset was determined just prior to the next pulse.

Data were digitized using a fast data acquisition card (National Instruments PCI-6133, 14-bit resolution, 2.5 MS/s/ch simultaneous sampling rate) connected to a laptop computer via a PCMCIA-to-PCI expansion unit (Magma CB4DRQ) and controlled by software written in LabVIEW. Because of their large number, the acquired ring-down decay traces were co-added to produce data at the desired time resolution (typically 1 s) prior to fitting to the parameters of a first exponential decay expression. Typically, ring-down time constants for dry zero air at 450 Torr of pressure were in the range of 60–65 μ s.

For comparison with the Nd:YAG laser system, the two blue diode CRDS cells were set up in series with those of the green Nd:YAG system. This ensured that the sample composition, pressure, and temperature were as similar as possible in the ring-down cells; the only systematic difference was due to additional dilution from purge flow. The two TD-CRDS instruments were operated using independent laser modulation and data acquisition systems.

Chemiluminescence Measurements of NO and NO_y. Mixing ratios of NO and NO_y were monitored using a commercial NO_y chemiluminescence (CL) analyzer (Thermo Scientific, model 42iTL). This instrument utilizes a molybdenum converter heated to 325 °C to convert the various NO_y species to NO, which is quantified by NO–O₃ chemiluminescence. An automated valve is used to switch between NO_y and (background) NO. The manufacturer-specified detection limit of the CL analyzer is 50 pptv over a 120 s averaging time. Corrections of the NO/NO_y data due to varying concentrations of water vapor (which affects the sensitivity of the CL measurement) were not necessary, since a common source of zero air was used as makeup gas in all experiments.

The calibration of the NO/NO_y CL instrument was periodically verified using a NO/N₂ calibration standard (Praxair, 2.8 or 99.5 ppm by volume (ppmv, 10^{-6}), certified) and a NO₂/air standard (Praxair, 120 ppmv, certified). The output of these cylinders was diluted with zero air, with the flows monitored by mass flow controllers. The amount of NO₂ delivered was verified by simultaneous CRDS measurements.

Synthesis of PAN Standards. The synthetic procedure (J. Roberts, personal communication) is based on the methods of Nielsen and Gaffney.^{20,21} PAN and PPN were synthesized from the corresponding peroxy-carboxylic acid, generated by reaction of H₂O₂ with acetic or propionic anhydride, respectively. The peroxy-carboxylic acid was then reacted with a mixture of HNO₃/H₂SO₄ at 0 °C and stored in tridecane in a freezer until use. Dilute gas mixtures of PAN or PPN were generated using a diffusion source stored in an ice/water bath whose output was diluted in ultrapure (zero) air. The purity of the PAN standards was verified by FT-IR spectroscopy; the PAN standard coemitted 3% HNO₃, 3% tridecane, and 2% acetic acid as impurities (percentages relative to PAN).

RESULTS AND DISCUSSION

Blue Diode Laser Spectroscopy of Nitrogen Dioxide. The diode laser's peak wavelength and output power are dependent on the current driving the diode, which in our system is controlled by a "control voltage" in the range of 0–1 V. Figure 2 shows normalized emission profiles of the blue diode laser at 0.5 and 1.0 V square-wave modulation amplitude (50% duty cycle), measured at the far end of the CRDS cell with the aid of a fiber-coupled miniature spectrometer (Ocean Optics USB 2000, integration time 4 ms, 500 spectra averaged) whose wavelength scale was calibrated using the output of a Hg pen ray lamp. Superimposed is the NO₂ absorption spectrum²² in this spectral region. The power dependence of the diode emission on the offset voltage is shown as an inset.

The emission of the diode is fairly broad, with a full width at half-maximum of 1.6 nm. As discussed by Fuchs et al.,¹² the width of the emission profile enables on-axis coupling of the diode output to the high-finesse ring-down cavity, because the laser line width encompasses many cavity modes. This in turn implies that "mode-

(20) Nielsen, T.; Hansen, A. M.; Thomsen, E. L. *Atmos. Environ.* **1982**, *16*, 2447–2450.

(21) Gaffney, J. S.; Fajer, R.; Senum, G. I. *Atmos. Environ.* **1984**, *18*, 215–218.

(22) Vandaele, A. C.; Hermans, C.; Fally, S.; Carleer, M.; Colin, R.; Merienne, M. F.; Jenouvrier, A.; Coquart, B. *J. Geophys. Res., [Atmos.]* **2002**, *107*, 4348–4360.

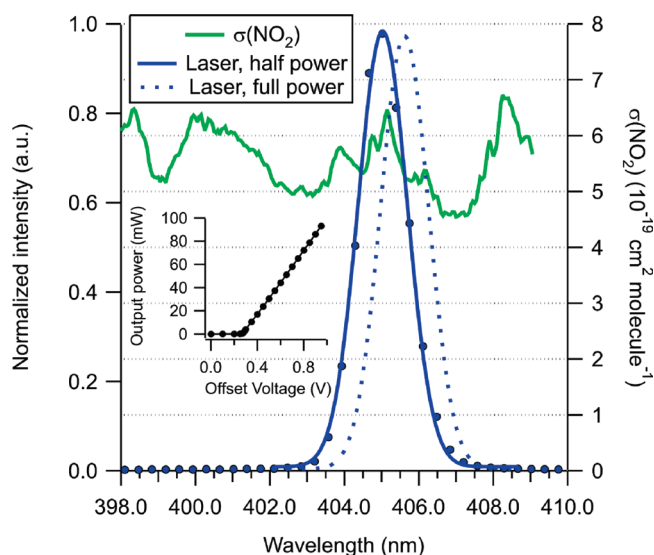


Figure 2. Emission profile of the blue diode laser at 50% and 100% power. The emission is broad (1.6 nm fwhm), facilitating on-axis coupling of the laser light to the high-finesse ring-down cavity. Superimposed (right-hand axis) is the NO_2 absorption spectrum in this spectral region.²² The NO_2 spectrum exhibits considerable structure, with features that are narrower than the line width of the laser. At the lower laser power, the absorption cross-section is approximately 20% larger than at maximum laser power.

beating" between multiple cavity modes is not expected. The NO_2 absorption spectrum exhibits structure over this range and varies between 4.5×10^{-19} and $6.5 \times 10^{-19} \text{ cm}^2 \text{ molecule}^{-1}$ (average $5.3 \times 10^{-19} \text{ cm}^2 \text{ molecule}^{-1}$). Thus, the photons experience different degrees of attenuation inside the ring-down cavity depending on their wavelength, as the absorption fine structure is smaller than the line width of the light inside the cavity. As pointed out by Zalicki and Zare,²³ this can potentially lead to non-first-order exponential ring-down decay traces and to problems with quantitative absorption measurements. However, we only observed first-order exponential ring-down decay traces (Figure 3), which indicates that this effect is negligible and that the perturbation by the fine structure of the NO_2 spectrum is sufficiently small to not pose a significant problem for quantitative measurements.

When the modulation amplitude is increased from 0.5 to 1.0 V, the peak center shifts from 405.0 to 405.6 nm (Figure 2), and the power is increased 3-fold. The increased output power bears little advantage in a CRDS experiment because the ring-down decay time constants do not depend on the intensity. Operating this particular diode at the higher output power is actually a disadvantage, as the NO_2 absorption cross-section decreases by about 20%. On the basis of the data shown in Figure 2, effective absorption cross-sections of $5.92 \times 10^{-19} \text{ cm}^2 \text{ molecule}^{-1}$ at half laser power and $5.20 \times 10^{-19} \text{ cm}^2 \text{ molecule}^{-1}$ at full diode power are predicted.

As is the case for the 532 nm instrument, the NO_2 absorption cross-section at 405 nm has also been reported to be slightly pressure- and temperature-dependent.¹⁹ We measured NO_2 mixing ratios (up to several 100 ppbv in zero air) in both the sample and reference channels and obtained a slope (sample/reference) of 1.007. The observed difference is less than the

combined uncertainties of pressure, temperature, and flow calibrations in both the sample and reference channels; we thus could not tell with certainty if this difference is indeed due to a small difference in the absorption cross-sections. Since the slightly greater response in the sample channel was highly reproducible, all data in the heated channel were scaled by this correction factor to improve the accuracy of the PAN measurement.

Simultaneous Measurements of PAN by the 532 and 405 nm TD-CRDS Instruments. To calibrate the 405 nm TD-CRDS instrument (i.e., to determine the effective absorption cross-section experimentally) and to validate the method, the two TD-CRDS instruments were connected in series, monitoring the same air. Figure 4 shows a time series of simultaneous measurements by the 532 and 405 nm TD-CRDS instruments of a mixture of NO_2 and PAN eluted from the diffusion source. The mixing ratio of PAN emitted from the source was varied by changing the flow rate of the dilution gas (zero air in this case). The output of the diffusion source was periodically bypassed, resulting in both instruments sampling only zero air (shown as a gray underlay).

The top two panels of Figure 4 show the ring-down time constants τ and τ_0 (interpolated from the times when the source was bypassed) in both the heated and reference channels. The ring-down time constants of the 405 nm instrument were considerably smaller (approximately 60 μs) than those at 532 nm (approximately 200 μs), mainly because of the larger Rayleigh scattering cross-section in the blue region of the electromagnetic spectrum. The relative precision of the 405 nm data is higher than that of the 532 nm data because of the larger number of ring-down decay traces averaged (750 vs 20).

The third panel shows the mixing ratios, derived from the number density calculated using eq 6 and the ideal gas law. For the 405 nm instrument, we used an effective cross-section of $6.1 \times 10^{-19} \text{ cm}^2 \text{ molecule}^{-1}$, which gave the best correlation with the 532 nm data (Figure 5). This experimentally determined cross-section is 3% greater than predicted; given the combined uncertainties of all the constants (e.g., NO_2 absorption cross-section at 532 nm) and measurements (i.e., of pressures, temperatures, and flow rates) going into the ΣPAN measurements, the level of agreement observed is excellent. With the 405 nm cross-section of $6.1 \times 10^{-19} \text{ cm}^2 \text{ molecule}^{-1}$, the NO_2 measurements in the reference channels (Figure 4C) are also in excellent quantitative agreement.

The $\text{NO}_2 + \Sigma\text{PAN}$ measurements in the sample channels are slightly lower in the 405 nm instrument because of (a) higher dilution from the mirror purge flows ($3 \times 50 \text{ sccm}$ vs $1 \times 50 \text{ sccm}$) and (b) partial recombination of the thermal dissociation products, PA radical and NO_2 (reaction 3) due to the longer residence time. Figure 4D shows the PAN mixing ratios measured by the two instruments. In this plot, the 405 nm PAN data were scaled up by a factor of 1.06 to account for the increased dilution by purge flow and greater extent of recombination. The rate of the recombination reaction is approximately second order in the PAN concentration present prior to thermal dissociation; its effects are thus more easily observed at high concentration. This is evident in the time series: The 405 nm measurement is considerably below the 532 nm measurement at 16:30, when the

(23) Zalicki, P.; Zare, R. N. *J. Chem. Phys.* **1995**, *102*, 2708–2717.

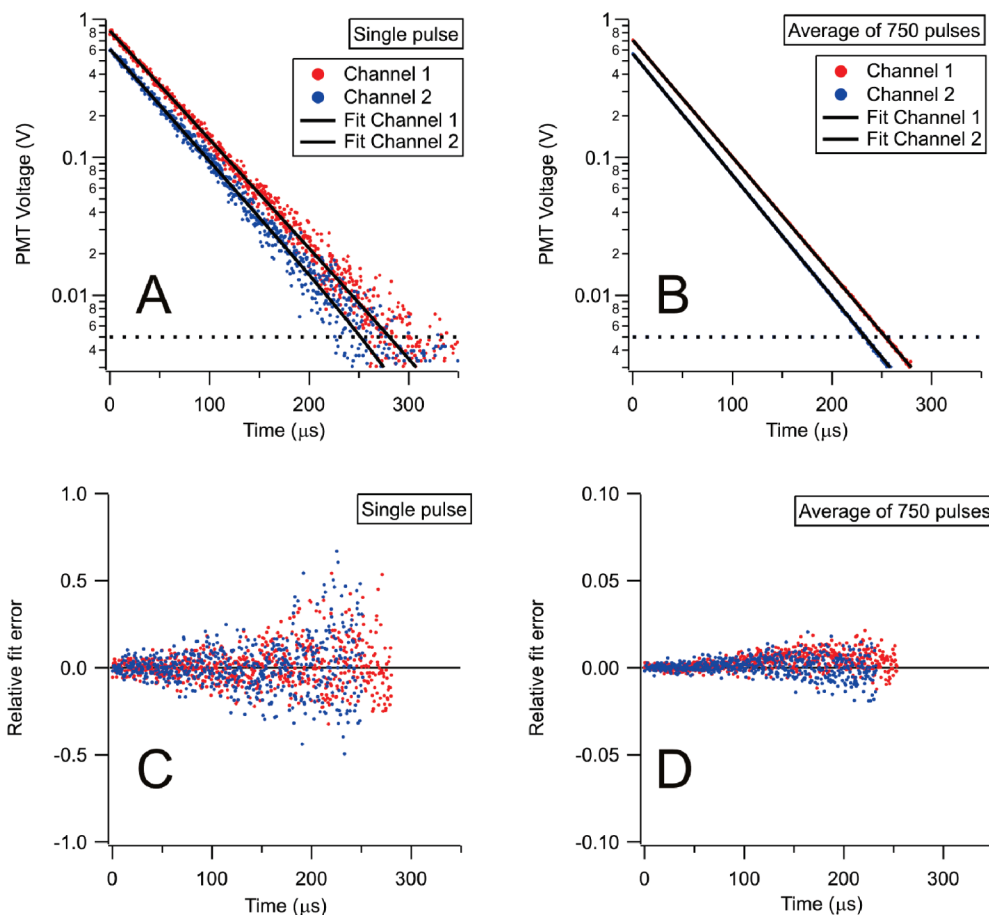


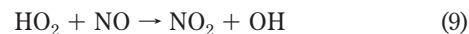
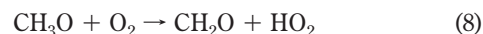
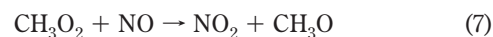
Figure 3. Observed blue diode laser CRDS decay traces and residuals to first-order exponential fits of the form $A_0 + A_1 \exp(-(t/\tau))$, where A_0 , A_1 , and τ are fitting parameters and t is time. For clarity, PMT offsets of +9.2 mV (channel 1) and +5.7 mV (channel 2) have been subtracted before presentation (i.e., A_0 has been forced to zero). The left-hand panels show “single shots”, whereas the right-hand panels show 750 trace averages. A non-first-order decay is possible due to the structured NO_2 absorption spectrum²³ but is not observed.

PAN concentration briefly peaks. The data shown in Figure 4 demonstrate that the 405 nm TD-CRDS instrument can be used as an alternative to the 532 nm TD-CRDS instrument to monitor NO_2 and ΣPAN in laboratory-generated samples.

Characterization of Interferences. The results presented to this point have so far included only peroxyacyl nitrate (either PAN or PPN) in zero air. The instrument is therefore suitable as a universal ΣPAN detector in laboratory experiments. The ultimate goal, though, are measurements of ΣPAN in an ambient air matrix. Ambient air contains a variety of species that can potentially interfere with the thermal conversion of ΣPAN to NO_2 . Aerosols, which add to optical extinction at 405 nm, can be removed by using an in-line Teflon filter. We verified that the Teflon filter (Pall) housed in a polycarbonate filter holder does not remove PAN (data not shown). We also investigated several potential interfering trace gases: water, ozone, nitric oxide, and nitrogen dioxide. Of these, only the latter two showed a non-negligible effect. Water is a known interference in the measurement of NO_2 by blue diode CRDS.¹² It does not, however, interfere with the thermal conversion efficiency; i.e., the ΣPAN signal is unaffected by addition of water (data not shown). Ozone was also added (up to 150 ppbv), but no significant effect was observed in either dry or humidified air (data not shown).

Figure 6 demonstrates the effect of adding NO_2 (top panel) or NO (bottom panel). The results for adding NO_2 are identical

to our previous measurements using the green Nd:YAG TD-CRDS instrument (eq 7b in ref 10) and are rationalized by an enhancement of the recombination reaction (3). Addition of NO leads to a nonlinear signal enhancement via reaction 4 and further oxidation of NO by the following reactions:



Several experiments were carried out at a variety of PAN and PPN mixing ratios. The signal amplification due to NO was well-reproduced by a second-order polynomial:

$$\Sigma\text{PAN}_{\text{obs}}/\Sigma\text{PAN} = (1 + [(3.94 \pm 0.03) \times 10^{-2}][\text{NO}] - [(1.69 \pm 0.03) \times 10^{-4}][\text{NO}]^2) \quad (10)$$

where $[\text{NO}]$ is in units of ppbv.

Figures of Merit and Comparisons with Existing Instruments. Table 1 gives a summary of the figures of merit of the current blue diode TD-CRDS instrument and of other PAN instruments described in the literature. For the blue diode TD-

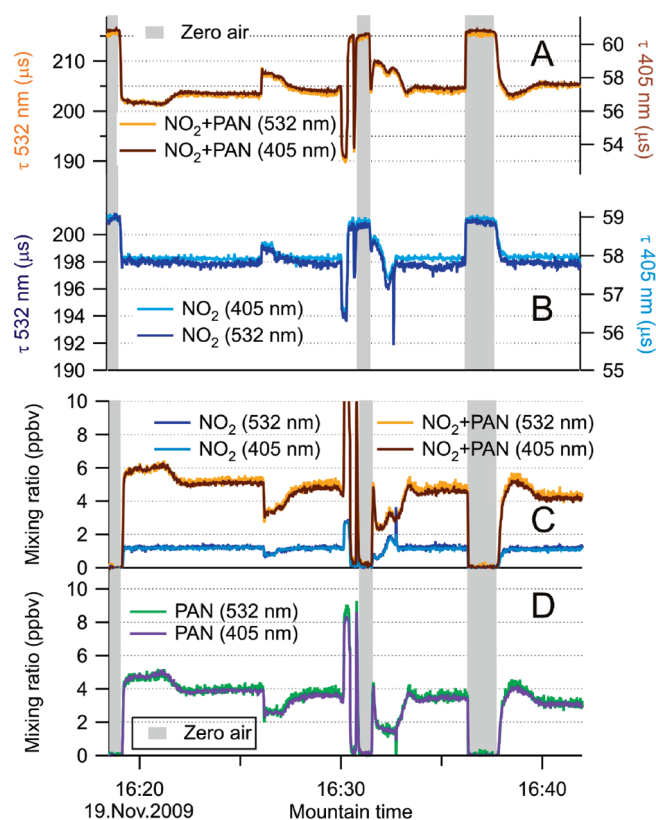


Figure 4. Simultaneous measurements of mixtures of PAN and NO₂ in zero air by the blue diode laser and green Nd:YAG TD-CRDS instruments connected in series. Observed ring-down time constants for the heated, sample, channels monitoring NO₂ + ΣPAN are shown in panel A, and those of the ambient-temperature, reference, channels monitoring NO₂ in panel B. The gray underlay identifies periods during which both instruments sampled zero air only. The concentrations were changed by varying the flow rates through the diffusion source. In all cases, the ring-down time constants of the two TD-CRDS instruments are well-correlated. Panel C shows the derived mixing ratios for the ambient and heated cells, respectively. Panel D shows the PAN mixing ratios derived by subtraction of the data shown in panel C.

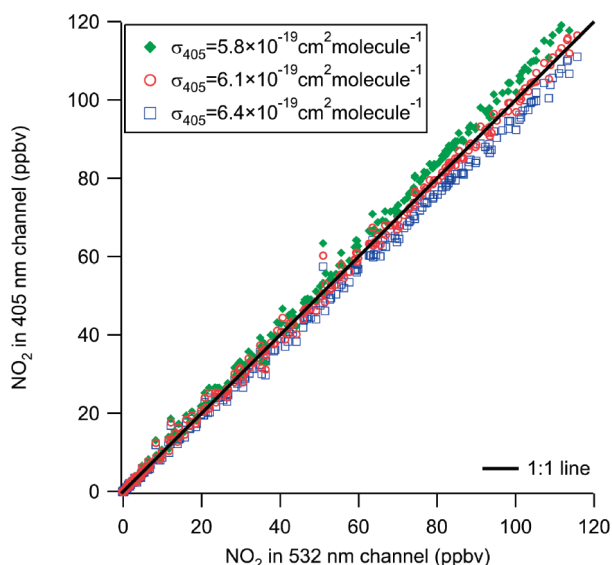


Figure 5. Determination of the effective NO₂ absorption cross-section at 405 nm.

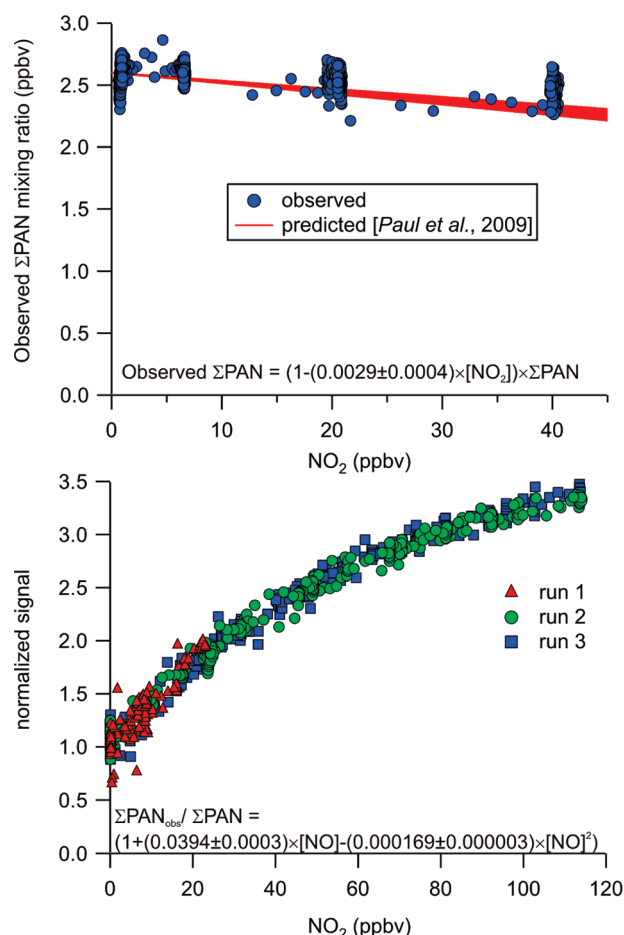


Figure 6. Interference tests. The top panel shows the effect of NO₂ addition on the ΣPAN signal, which leads to a signal reduction. The bottom panel shows the effect of adding NO, which leads to a signal amplification.

CRDS instrument in its current form, the 1σ precision of 1 s data is 30 pptv for single-channel data and 60 pptv for ΣPAN data.

This represents a considerable improvement (factor of 2) compared to the previous, 532 nm, TD-CRDS instrument.¹⁰ However, the level of improvement is not as large as one might have expected, given that the absorption cross-section is 4 times larger at 405 nm and that a 750/20 = 37.5-fold greater number of ring-down traces are averaged in a 1 s interval. The greater number of ring-down decay traces alone should have yielded an approximately $\sqrt{37} \approx 6$ -fold improvement, but only an improvement by a factor of 2 was realized. The larger number of ring-down traces averaged should have also improved the relative precision of the fit error, i.e., the precision with which the ring-down decay constants are determined. These were $0.010/65 = 1.5 \times 10^{-4}$ and $0.05/175 = 3 \times 10^{-4}$, respectively, and thus also “only” differed by a factor of 2. These results suggest that additional sources of noise exist in the cw blue diode laser system that do not, or not to the same extent, exist in the pulsed Nd:YAG system. It is not known with certainty what these noise sources are; possibly, the additional noise is caused by small pulse-to-pulse variation of the blue diode laser wavelength. The latter is highly sensitive to the laser head temperature and current; the stability of neither was monitored. In contrast, the output wavelength of the pulsed Nd:YAG laser is likely more stable and reproducible, yielding a higher measurement preci-

Table 1. Overview of Figures of Merit for Σ PAN (PAN) Measurement Techniques

parameter	GC-ECD ⁴	TD-LIF ^{8,9,a}	TD-CIMS ⁷	Nd:YAG TD-CRDS ¹⁰	blue diode TD-CRDS (this work)
precision (1 σ , 1 s)	n/a	16 pptv	≤ 1 pptv	100 pptv	60 pptv
precision (1 σ , 1 min)	≤ 1 pptv	2 pptv	n/d	30 pptv	20 pptv
calibration	external	external	external	absolute	absolute
NO interference	no	+	–, internal standard required	+	+
NO ₂ interference	no	–	–, internal standard required	–	–
speciation	yes	no	yes	no	no

^a Values calculated on the basis of the \sqrt{n} dependence from the stated precision: 30 ppt (2 σ), 10 s.

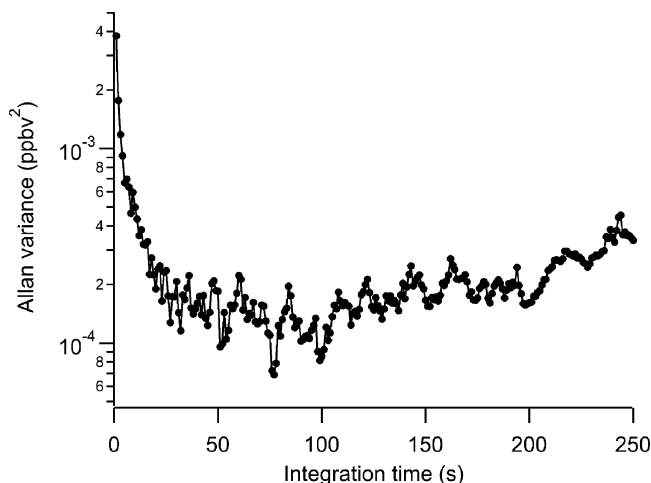


Figure 7. Allan variance plot of Σ PAN data acquired by TD-CRDS. The minimum indicates the optimum integration time (approximately 1 min).

sion. Further, the detection limit of a CRDS instrument depends on the ability to distinguish between the signal and background ring-down time constants, τ and τ_0 . The larger ring-down time constants observed in the 532 nm instrument (due to the lower Rayleigh scattering cross-section) thus likely partially offset the other advantages of the blue laser instrument.

An Allan variance²⁴ plot (Figure 7) indicates an optimum integration time of about 1 min (under flow) for the TD-CRDS instrument; the 1 σ precision of 1 min data then improves to 20 pptv for Σ PAN. For the Nd:YAG system, the optimum integration time was determined to be 5 min. This again suggests the presence of one more additional noise source in the blue diode laser system that is not present in the Nd:YAG TD-CRDS instrument. In spite of this, the blue diode TD-CRDS instrument still outperforms the Nd:YAG system overall in terms of instrumental precision. Since the two TD-CRDS instruments are tied to the same calibration and utilize identical inlets, their (slope) accuracy (approximately 4% limited mainly by uncertainties in the knowledge of the NO₂ absorption cross-section)^{11,18} and linear dynamic range (which for dilute PAN samples extends from the detection to about 10 ppbv) are identical.

The performance of the blue diode laser TD-CRDS instrument for NO₂ in its present form is a factor of 3 worse than that reported by Fuchs et al., who reported a 1 σ precision of 11 pptv for 1 s data.¹² The main difference between the Fuchs et al. system and ours is that the former averages 1600 traces

and determines the ring-down constants by fitting to a single-exponential decay with three parameters (time constant, amplitude, offset); in our system, the offset is measured explicitly between traces, and only the time constant and amplitude are fitted to an average of 750 traces. This suggests that the computationally more expensive approach chosen by Fuchs et al. is advantageous. We will likely implement the improved fitting algorithm in future versions of the blue diode TD-CRDS instrument.

The instrument sensitivity is somewhat worse than that of the TD-LIF instrument and almost 2 orders of magnitude worse than that of the TD-CIMS instrument and, at the lower time resolution, that of the GC-ECD instrument. It is thus unlikely that TD-CRDS will replace any of the existing techniques any time soon. However, the TD-CRDS instrument differs in that its measurements can be considered absolute. In contrast to existing, more sensitive, measurement techniques, TD-CRDS offers the distinct advantage of not having to rely on external calibration nor on an internal standard. This is a considerable advantage as the synthesis and delivery of high-purity samples of PANs are very challenging,^{25,26} requiring combinations of laborious extractions and calibrations using preparative GC. The synthesis of PAN calibration standards is required for GC-ECD and TD-CIMS, as these techniques exhibit different response factors for different PANs.^{4,27} Because TD-CRDS exhibits the same response factor to all PANs, it is a valuable addition to the available suite of measurement techniques available to the atmospheric chemistry community.

Applications. Even though TD-CRDS is still bested by the other measurement techniques listed in Table 1, the measurement speed and sensitivity already suffice for many applications. For example, the TD-CRDS instrument can be used as a universal detector to monitor Σ PAN mixing ratios at near-ambient levels in heterogeneous uptake experiments using either a coated wall reactor or an aerosol flow tube. In fact, such experiments are already under way in our laboratory.

The TD-CRDS measurement precision also suffices for quantification of Σ PAN at levels encountered in polluted (i.e., urban) environments, but falls somewhat short of levels encountered in

(24) Werle, P.; Mücke, R.; Slemr, F. *Appl. Phys. B: Photophys. Laser Chem.* **1993**, 57, 131–139.

(25) Roberts, J. M.; Williams, J.; Baumann, K.; Buhr, M. P.; Goldan, P. D.; Holloway, J.; Hubler, G.; Kuster, W. C.; McKeen, S. A.; Ryerson, T. B.; Trainer, M.; Williams, E. J.; Fehsenfeld, F. C.; Bertman, S. B.; Nouaime, G.; Seaver, C.; Grodzinsky, G.; Rodgers, M.; Young, V. L. *J. Geophys. Res., [Atmos.]* **1998**, 103, 22473–22490.

(26) Tanimoto, H.; Akimoto, H. *Geophys. Res. Lett.* **2001**, 28, 2831–2834.

(27) LaFranchi, B. W.; Wolfe, G. M.; Thornton, J. A.; Harrold, S. A.; Browne, E. C.; Min, K. E.; Wooldridge, P. J.; Gilman, J. B.; Kuster, W. C.; Goldan, P. D.; de Gouw, J. A.; McKay, M.; Goldstein, A. H.; Ren, X.; Mao, J.; Cohen, R. C. *Atmos. Chem. Phys.* **2009**, 9, 7623–7641.

the remote troposphere. To facilitate such measurements, the detection limit of the TD-CRDS instrument can be further improved by (1) optimizing the NO₂ detection following the improved fitting routine described by Fuchs et al.¹² and (2) deliberately amplifying the signal by addition of a high and constant background of NO (e.g., 100 ppbv). If both measures are taken, a future gain in sensitivity by about 1 order of magnitude can be anticipated. The major interferences expected in ambient air are already well-characterized and can be corrected for using simple polynomial expressions. Furthermore, the high acquisition speed of the TD-CRDS instrument (>10 Hz) will enable Σ PAN flux measurements by Eddy covariance.²⁸

CONCLUSIONS

A novel thermal dissociation cavity ring-down spectrometer utilizing a 405 nm cw diode laser for measurement of the total peroxy nitrate abundances at ambient concentration levels has been described. The upgrade from a Nd:YAG laser to a blue diode laser is an important milestone toward developing a field-ready TD-CRDS instrument, as it improves the sensitivity and reduces

the size, weight, cost, and maintenance requirements. For example, the Nd:YAG laser requires regular exchange of flash lamps and uses an external control unit containing deionized water that can freeze in field deployments. In contrast, the blue diode is essentially a maintenance-free compact turnkey device—at less than a quarter of the acquisition price of a Nd:YAG laser. The advantage of TD-CRDS over other existing PAN measurement techniques such as GC-ECD or TD-CIMS is that its measurement can be considered absolute; i.e., it does not need to rely on either external calibration nor does it require an internal standard. Potential applications of this new method include laboratory and field measurements.

ACKNOWLEDGMENT

This work was financially supported by the National Science and Engineering Research Council of Canada (NSERC) in the form of a Discovery grant, by an Alberta Ingenuity Fund New Faculty award, and by the University of Calgary Faculty of Science, who contributed startup funding.

(28) Turnipseed, A. A.; Huey, L. G.; Nemitz, E.; Stickel, R.; Higgs, J.; Tanner, D. J.; Slusher, D. L.; Sparks, J. P.; Flocke, F.; Guenther, A. J. *Geophys. Res., [Atmos.]* **2006**, *111*, D09304.

Received for review June 1, 2010. Accepted June 29, 2010.

AC101441Z